Journal of Power Sources 195 (2010) 6101–6107

Contents lists available at ScienceDirect

Journal of Power Sources

journal homepage: www.elsevier.com/locate/jpowsour

Effects of synthesis temperature and precursor composition on the crystal structure, morphology, and electrode activity of 1D nanostructured manganese oxides

In Young Kim[a], Sun Hee Lee[a], Hyung-Wook Ha[a], Tae Woo Kim[a], Yoon Soo Han[b], Jin Kyu Kang[b], Dong Ha Lee[b], Seong-Ju Hwang[a,*]

[a] Center for Intelligent Nano-Bio Materials (CINBM), Department of Chemistry and Nano Sciences, Ewha Womans University, Seoul 120-750, Republic of Korea
[b] Daegu Gyeongbuk Institute of Science and Technology (DGIST), Daegu, Republic of Korea

ARTICLE INFO

Article history:
Received 15 October 2009
Received in revised form
10 November 2009
Accepted 11 November 2009
Available online 18 November 2009

Keywords:
Precursor composition
Reaction temperature
1D nanostructured manganese oxide
Crystal structure
Morphology
Electrode activity

ABSTRACT

1D nanostructured manganese oxides are prepared by oxidation reaction of precursor $LiMn_{2-x}Cr_xO_4$ microcrystals under hydrothermal condition. The crystal structure and morphology of the obtained manganese oxides are strongly dependent on the reaction condition and the chemical composition of the precursors. The α-MnO_2 nanowires are prepared by reaction at 120 °C, and their aspect ratios decrease with the Cr content in the precursor. Treating precursors with persulfate ions at 160–180 °C yields the β-MnO_2 nanorods for the precursors $LiMn_{2-x}Cr_xO_4$ with lower Cr content and the α-MnO_2 nanowires for the precursors with higher Cr content. The structure dependence of the products on the Cr content in the precursors is related to the high octahedral site stabilization energy of Cr^{3+} ions and/or to the increase of Mn valence state upon Cr substitution. The increase of Cr content in the precursors degrades the electrode performance for the manganates prepared at 160 °C but improves electrode activity for those prepared at 180 °C. This observation can be explained by the structural variation and chromium substitution of the hydrothermally treated manganates. We conclude that the use of spinel $LiMn_{2-x}Cr_xO_4$ as precursors provides an effective way to synthesize 1D nanostructured manganate with tailored crystal structure and morphology.

1. Introduction

During the last several decades, manganese oxides have attracted particular attention as promising electrode materials for lithium secondary batteries because of their many advantages such as excellent electrochemical activity, cheap price, facile synthesis, and low toxicity [1]. Compared with microcrystalline electrode materials, nanocrystalline manganese oxides show many advantages including large discharge capacity, high cyclability, excellent rate characteristics, etc. [2–5]. One-dimensional (1D) manganese oxide nanowires/nanorods having diverse crystal structures have been synthesized through the hydrothermal reaction of manganese-containing precursors [6–13]. Their anisotropic morphology and expanded surface area would guarantee superior rate- and cycle-characteristics over the bulk counterparts. The chemical substitution for the 1D nanostructured manganese oxides could be achieved by adopting chemically substituted manganese oxide microcrystals as precursors [9,10]. The structural and electrochemical properties of the product manganates are expected to strongly depend on the chemical composition and Mn valence of the solid-state precursor and the reaction temperature, as well. To date, however, there has been no systematic study on the effects of these factors on the crystal structure, morphology, and electrochemical property of 1D nanostructured manganese oxides. Understanding of these effects is quite informative in preparing nanostructured manganese oxide electrodes with improved functionality. For this purpose, the spinel-structured lithium manganate is one of the most suitable precursors since the chemical composition and Mn valence in this phase can be easily modified by cation substitution [1,14].

In this study, we synthesized 1D nanostructured manganese oxides with various crystal structures and chemical compositions by treating the precursor $LiMn_{2-x}Cr_xO_4$ spinel oxides with persulfate ions under hydrothermal condition. The structural, morphological, and bonding characteristics of the obtained materials were examined to probe their correlation with the reaction condition and precursor composition. Also, we investigated the evolution

* Corresponding author at: Center for Intelligent Nano-Bio Materials (CINBM), Department of Chemistry and Nano Sciences, Ewha Womans University, 11-1, Daehyun-dong, Seodaemun-gu, Seoul, Republic of Korea. Tel.: +82 2 3277 4370; fax: +82 2 3277 3419.
E-mail address: hwangsju@ewha.ac.kr (S.-J. Hwang).

0378-7753/$ – see front matter © 2009 Elsevier B.V. All rights reserved.
doi:10.1016/j.jpowsour.2009.11.053

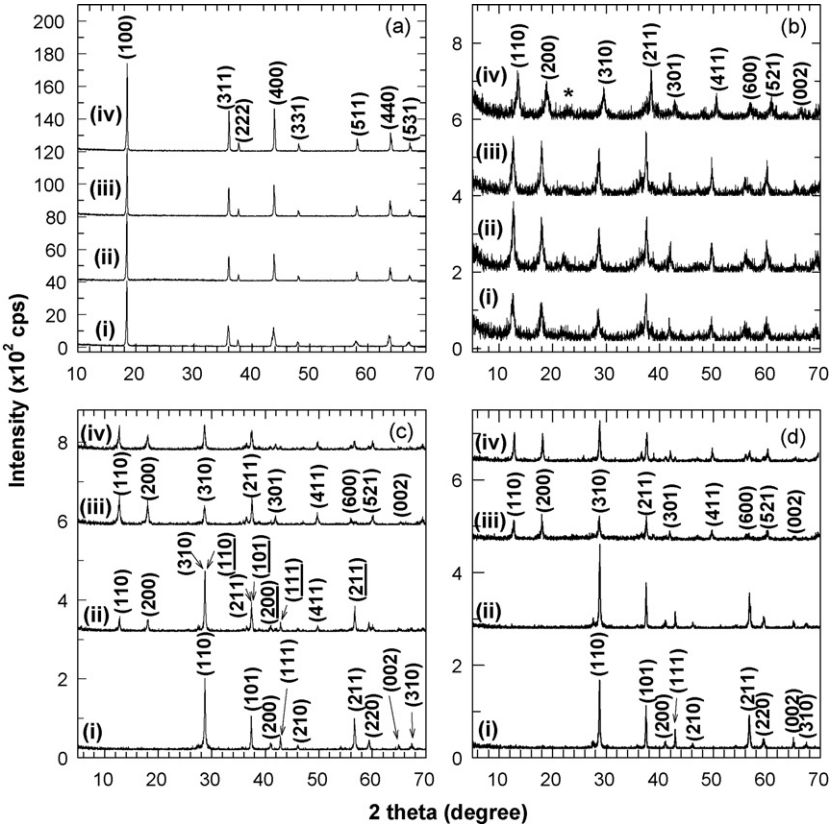

Fig. 1. Powder XRD patterns of (a) the precursor spinel $LiMn_{2-x}Cr_xO_4$ and their hydrothermally treated derivatives at (b) 120 °C, (c) 160 °C, and (d) 180 °C. The data (i), (ii), (iii), and (iv) correspond to the samples with $x = 0$, 0.1, 0.3, and 0.5, respectively. In (b), the asterisk represents the (1 1 0) reflection of γ-MnO_2 phase. In (c)-(ii), miller indices of Bragg reflections corresponding to the β-MnO_2 phase are underlined.

of the electrochemical activity of 1D nanostructured manganese oxides caused by structural transition and cation substitution.

2. Experimental

2.1. Synthesis

The precursors of cubic spinel $LiMn_{2-x}Cr_xO_4$ ($x = 0$, 0.1, 0.3, and 0.5) were prepared by heat-treatment of the stoichiometric mixture of Li_2CO_3, Cr_2O_3, and Mn_2O_3 at 730–750 °C in ambient atmosphere [14]. To synthesize 1D nanostructured manganese oxides, the precursors were reacted with 0.5 M aqueous solution of $(NH_4)_2S_2O_8$ at 120–180 °C for 36 h in Teflon-lined hydrothermal vessel. After the hydrothermal reaction, the hydrothermal vessel was cooled to room temperature. The obtained powders were washed thoroughly with distilled water and dried in oven.

2.2. Characterization

The structural variations of the precursor $LiMn_{2-x}Cr_xO_4$ during hydrothermal treatment with persulfate ions were probed with powder X-ray diffractometer, or XRD (Rigaku, $\lambda = 1.5418$ Å, 298 K). We used inductively coupled plasma, or ICP, spectrometry to determine the chemical compositions of the present nanostructured manganese oxides. The crystallite morphologies and cation compositions of these materials were probed using field emission-scanning electron microscopy, or FE-SEM (Jeol JSM-6700F equipped with an energy-dispersive X-ray spectrometer, or EDS). The crystal dimensions of the manganates were examined using high resolution-transmission electron microscopy, or HR-TEM (Jeol JEM-2100F, 200 kV). X-ray absorption spectroscopy, or XAS, experiments were carried out with the extended X-ray absorption fine structure, or EXAFS, facility installed at the beam line 7C at the Pohang Accelerator Laboratory (PAL) in Korea. XAS data were collected at room temperature in a transmission mode using gas-ionization detectors. All the present spectra were calibrated by simultaneously measuring the spectrum of manganese or chromium metal foil. The data analysis for the experimental spectra was performed by the standard procedure reported previously [15].

2.3. Performance test as lithium intercalation electrode

Electrochemical measurements were performed with the cell of Li/1 M $LiPF_6$ in EC:DEC (50:50, v/v)/composite cathode, which was assembled in Ar-filled glove box. The composite cathode was prepared by mixing thoroughly 20 mg of active electrode material with 12 mg of conductive binder (i.e. 8 mg of teflonized acetylene black and 4 mg of graphite). All the experiments were carried out in a galvanostatic mode with a Maccor multichannel galvanostat/potentiostat. The measurements were performed in the voltage range of 1.0–4.4 V at a constant current density 20 mA g^{-1}.

3. Results and discussion

3.1. Powder XRD measurement

The powder XRD patterns of the precursors $LiMn_{2-x}Cr_xO_4$ ($x = 0$, 0.1, 0.3, and 0.5) and their hydrothermally treated derivatives are plotted in Fig. 1. All the precursor compounds show typical XRD patterns of cubic spinel lattice [1,14,16]. There is no Bragg reflection corresponding to impurity phase like Cr_2O_3, indicating

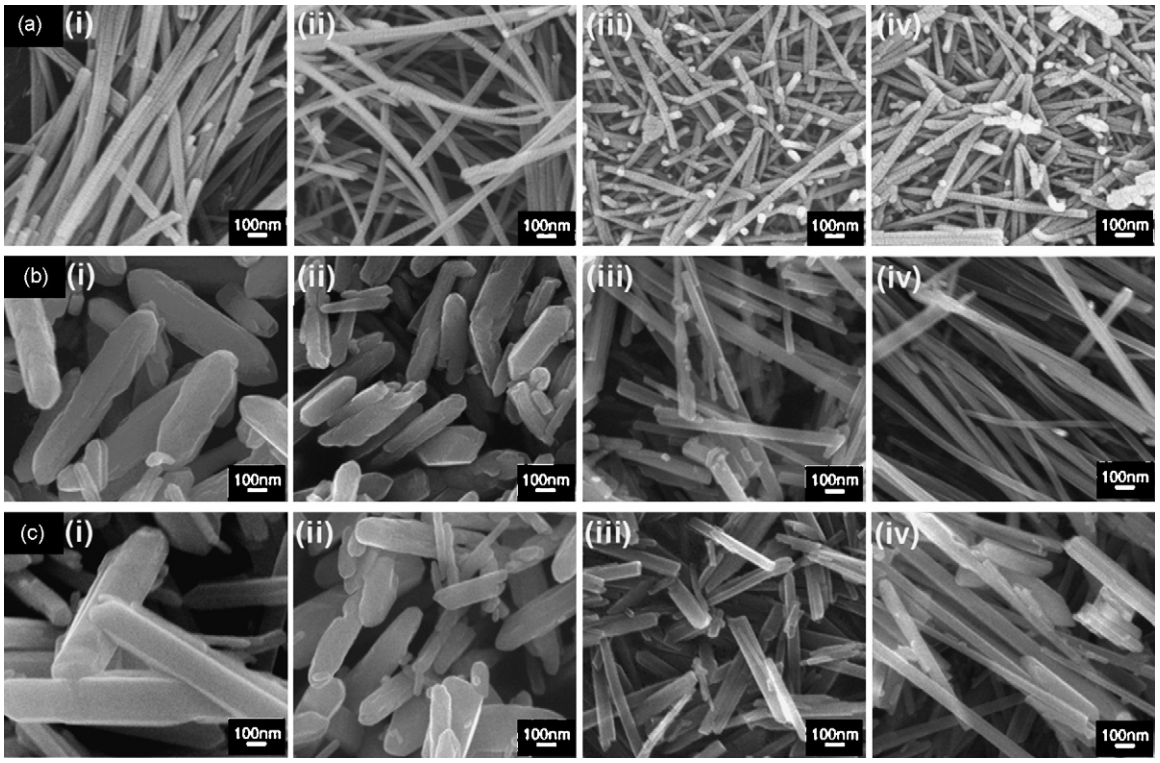

Fig. 2. FE-SEM images of 1D nanostructured manganese oxides prepared by hydrothermal treatment for the spinel $LiMn_{2-x}Cr_xO_4$ at (a) 120 °C, (b) 160 °C, and (c) 180 °C. The data (i), (ii), (iii), and (iv) correspond to the samples with $x = 0$, 0.1, 0.3, and 0.5, respectively.

the formation of pure cubic spinel $LiMn_{2-x}Cr_xO_4$ phase for the present Cr substitution range ($0 \le x \le 0.5$). Persulfate treatment of the precursors at 120 °C gives rise to the formation of the α-MnO_2 phase with a minor γ-MnO_2 phase. Conversely, the hydrothermal persulfate treatment at 160 °C produced β-MnO_2 phase with the precursor $LiMn_2O_4$. At the same temperature, the precursor $LiMn_{1.9}Cr_{0.1}O_4$ transformed into the mixed phase of α-MnO_2 and β-MnO_2. The pure α-MnO_2 phase was obtained with the precursors $LiMn_{2-x}Cr_xO_4$ with $x = 0.3$ and 0.5. At higher temperature of 180 °C, the hydrothermal persulfate treatments yielded the β-MnO_2 phase for the lightly Cr-substituted precursors with $x = 0$ and 0.1 or the α-MnO_2 phase for the heavily Cr-substituted precursors with $x = 0.3$ and 0.5 [17]. The present XRD results emphasize that the crystal structures of the hydrothermally treated derivatives are strongly dependent on the reaction temperature and chromium content in the precursors; the hydrothermal treatment at elevated temperatures prefers the formation of more densely packed structure, i.e. β-MnO_2, as reported previously [10]. The increase of Cr content in the precursor hinders the formation of the β-MnO_2 phase and hence this phase could not be obtained for the heavily Cr-substituted precursors. According to the report on the formation mechanism of 1D nanostructured manganese oxides [8], the intermediate layered crystallites are formed at the initial stage of hydrothermal reaction and then rolled into the nanowires/nanorods. Such morphological changes accompany structural transformation of layered MnO_2 into α-MnO_2 or β-MnO_2 structure [8]. This structural modification can occur via the migration of Mn ions into neighboring octahedral sites through interstitial tetrahedral sites [18]. Considering the high octahedral site stabilization energy of trivalent chromium ion with d^3 electronic configuration, this Cr^{3+} ion has a strong tendency to stay in the octahedral sites and to resist migration to interstitial sites. Such a fixation of chromium ions in the octahedral sites would hinder the migration of neighboring manganese ions, since the displacement of metal ions promotes the migration of adjacent metal ions by reducing the potential barrier for diffusion. As a consequence, the substitution of Cr^{3+} ions seems to prevent the transformation into the β-MnO_2 structure. Also, the partial replacement of Cr^{3+} ions for Mn^{3+}/Mn^{4+} ions in the spinel $LiMn^{3.5+}{}_2O_4$ increases the average oxidation state of remaining manganese ions. Since the 1D morphology can be created by the rolling and folding of the layered crystallites [8], the spinel $LiMn_{2-x}Cr_xO_4$ precursors with non-layered structure should be dissolved during the hydrothermal reaction and then recrystallized as intermediate layered crystallites. In this study, we confirmed the formation of intermediate layer-shaped crystallites during the hydrothermal reaction of the spinel lithium manganates (not shown here). The Mn^{3+} ions in the oxide lattice yield soluble Mn^{2+} and insoluble Mn^{4+} ions disproportionately [19]. Thus, the increase of Mn valency close to +4 during the Cr substitution would depress the solubility of solid-state precursor and hence retard the formation of the 1D nanostructured manganese oxide. Such a suspended formation of 1D nanostructured manganese oxide also prevents the transformation of layered MnO_2 structure to β-MnO_2 structure.

3.2. EDS, ICP, FE-SEM, and HR-TEM analyses

According to the EDS analysis, a small amount of Cr ions are incorporated into the nanostructured manganese oxides with the Cr/Mn ratio of 0.005–0.09 [20]. As the Cr content in the precursor increases, the concentration of chromium ion in the products becomes higher. The ICP analysis revealed that there are only a negligible amount of lithium ions in the hydrothermally treated derivatives, implying the severe loss of the lithium ions during the hydrothermal treatment.

The crystal morphology of the 1D nanostructured manganese oxides was examined with FE-SEM. As shown in Fig. 2, 1D nanowires with a diameter of ~30 nm and a length of several micrometers were obtained from the hydrothermal persulfate treatments of the precursors at 120 °C. As the Cr content in the pre-

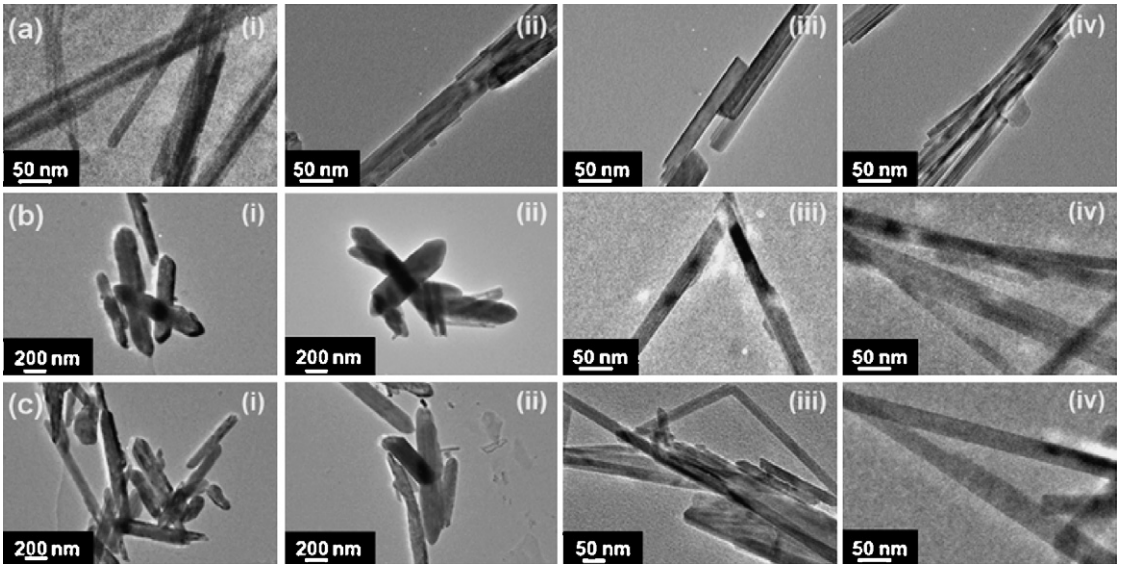

Fig. 3. HR-TEM images of 1D nanostructured manganese oxides prepared by hydrothermal treatment for the spinel $LiMn_{2-x}Cr_xO_4$ at (a) 120 °C, (b) 160 °C, and (c) 180 °C. The data (i), (ii), (iii), and (iv) correspond to the samples with $x = 0$, 0.1, 0.3, and 0.5, respectively.

cursors increases, the aspect ratio of the nanowires decreases. This can be understood as a result of the mismatch of ionic size between Cr^{3+} and Mn^{4+} ions, disturbing the effective crystal growth of α-MnO_2 phase [21]. After the hydrothermal reactions at 160–180 °C, the β-MnO_2-structured samples prepared with the lightly Cr-substituted precursors show 1D nanorod-type morphology with a diameter of ~100–300 nm and a length of several hundred nanometers. Conversely, the nanowires-like morphology with a higher aspect ratio could be observed for the α-MnO_2-structured samples prepared with the heavily Cr-substituted precursors. The higher aspect ratio of the α-MnO_2-structured materials can be attributed to the inherent growth pattern of this structure, preferring anisotropic growth into 1D morphology along the direction of 2×2 tunnels. That the β-MnO_2 structure is not anisotropic is reflected in the lower aspect ratio of the β-MnO_2-structured materials. The formation of the 1D nanostructures after the hydrothermal reaction was further evidenced by HR-TEM analysis. As illustrated in Fig. 3, the crystal dimensions of the nanostructured materials estimated from the HR-TEM results are very consistent with those from the FE-SEM data (Fig. 2).

3.3. Mn K- and Cr K-edge XANES analyses

Evolutions of the local atomic arrangement and electronic structure of Mn and Cr ions during the hydrothermal treatments were investigated with X-ray absorption near-edge structure, or XANES, spectroscopy at Mn K-edge and Cr K-edge. Fig. 4 represents the Mn K-edge XANES spectra of the precursors $LiMn_{2-x}Cr_xO_4$ ($0 \le x \le 0.5$) and their hydrothermally treated derivatives, compared with those of layered $LiMn_{0.9}Cr_{0.1}O_2$ and spinel-structured λ-MnO_2. The edge energies of the precursors are lower than that of the reference λ-$Mn^{4+}O_2$ but higher than that of $LiMn_{0.9}{}^{3+}Cr_{0.1}O_2$, reflecting the mixed oxidation states of Mn^{3+}/Mn^{4+} in these compounds. During the hydrothermal treatment with persulfate ions, the precursors commonly undergo a distinct blue-shift of edge energy close to that of the reference λ-$Mn^{4+}O_2$, highlighting the increase of Mn oxidation state. In pre-edge region, weak peaks P and P′ corresponding to dipole-forbidden $1s \rightarrow 3d$ transitions are detected for all the present materials [22]. Since the intensity of these features is proportional to the structural distortion from regular octahedral symmetry, the weak intensity of these pre-edge features provides the strong evidence for the stabilization of manganese ions in the centrosymmetric octahedral site [22]. The increase of spectral weight for the peak P′ reflects the increase of Mn oxidation state [22]. As shown in the inset of Fig. 4, the hydrothermal treatments enhance this peak for all the precursors, confirming the oxidation of manganese ions. All of the manganese oxides under investigation exhibit several main-edge peaks A, B, and C, which are accounted for by dipole-allowed $1s \rightarrow 4p$ transitions. All the nanostructured manganates demonstrate weaker intensity for the peaks A and B, compared with the bulk $LiMn_{2-x}Cr_xO_4$. Such weak and diffuse features of the main-edge peaks are characteristic of nanocrystalline metal oxide [22]. Also, the hydrothermal persulfate treatment causes remarkable spectral variations in the peak C whose intensity and sharpness are proportional to the relative concentration of edge-sharing over corner-sharing of MnO_6 octahedra [23]. As shown in Fig. 4, the precursor $LiMn_{2-x}Cr_xO_4$ materials display a sharp and intense peak C, which is very consistent with their spinel structures composed of edge-shared MnO_6 octahedra only. After the hydrothermal reactions, the peak C becomes broader and weaker than the precursors, confirming the structural transition to the α-MnO_2-type or β-MnO_2-type structure composed of the corner- and edge-sharing of MnO_6 octahedra. A closer inspection revealed that, regardless of reaction temperature, the hydrothermal treatments for the heavily Cr-substituted precursors with $x = 0.3$ and 0.5 induced the broadening of the peak C (Fig. 4c and d). The broad peak C is typical spectral feature of the α-MnO_2 phase [10]. In the lightly Cr-substituted manganate precursors with $x = 0$ and 0.1 (Fig. 4a and b), similar α-MnO_2-like feature is observed after the hydrothermal treatment at 120 °C. Conversely, β-MnO_2-like main-edge feature appears after the hydrothermal treatment at 160–180 °C. This finding is very consistent with the powder XRD results showing a strong dependence of the crystal structure of hydrothermally treated manganates on the reaction temperature (Fig. 1).

The chemical bonding nature of chromium ions in the nanostructured manganese oxides was examined with Cr K-edge XANES analysis. Since the concentration of chromium ions in the resulting nanostructures is quite low, XANES analysis was carried out for the most heavily Cr-substituted compounds with $x = 0.5$. Fig. 5 illustrates the Cr K-edge XANES spectra for the pristine $LiMn_{1.5}Cr_{0.5}O_4$ and its hydrothermally treated derivatives, and the reference Cr_2O_3. The edge energies of all the present compounds are almost identical to that of Cr_2O_3, suggesting the trivalent oxidation state of

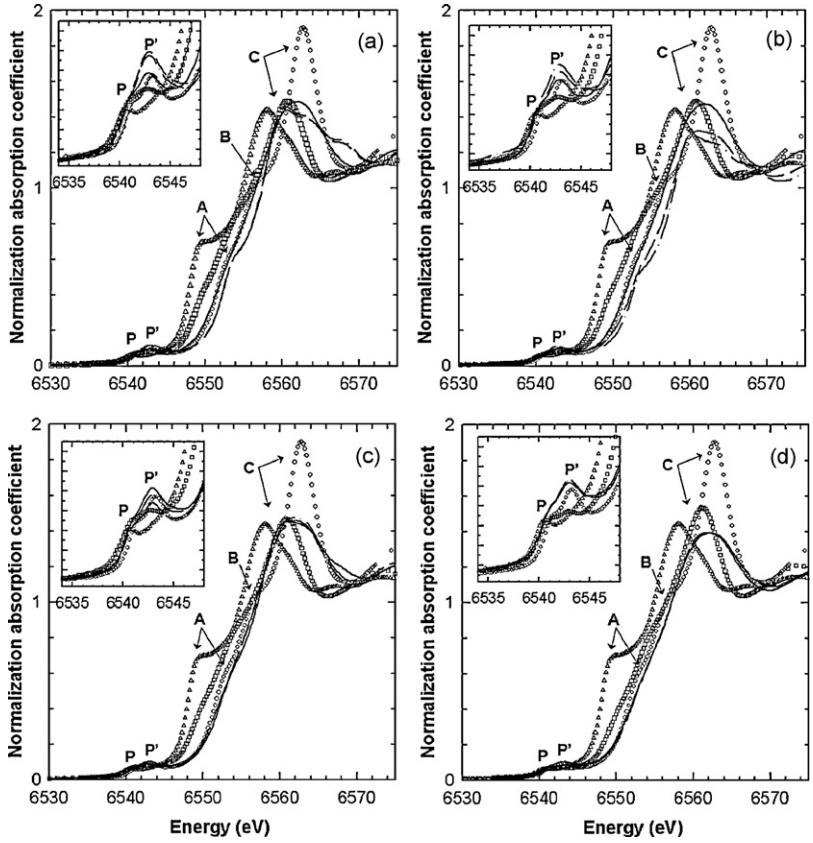

Fig. 4. Mn K-edge XANES spectra for the precursor spinel $LiMn_{2-x}Cr_xO_4$ (squares) with x = (a) 0, (b) 0.1, (c) 0.3, and (d) 0.5, and their hydrothermally treated derivatives at 120 °C (solid lines), 160 °C (dashed lines), and 180 °C (dot-dashed lines), and the references $LiMn_{0.9}Cr_{0.1}O_2$ (triangles) and λ-MnO_2 (circles). The insets provide expanded views of pre-edge spectra with the energy region of 6534–6548 eV.

chromium in these compounds. Like the Mn K-edge region, all the nanostructured materials show a weak pre-edge peak P related to the dipole-forbidden $1s \rightarrow 3d$ transition. This indicates the substitution of Cr ions for the octahedral Mn sites. In this Cr K-edge region, all the nanostructured manganese oxides exhibit nearly identical main-edge spectral features including the broad peak C, which are characteristic of α-MnO_2 phase. The present spectral features are quite similar to those in the corresponding Mn K-edge XANES data (Fig. 4d). The Cr K-edge XANES result can be considered as the strong evidence for the stabilization of chromium ions in the Mn sites of the α-MnO_2 lattice.

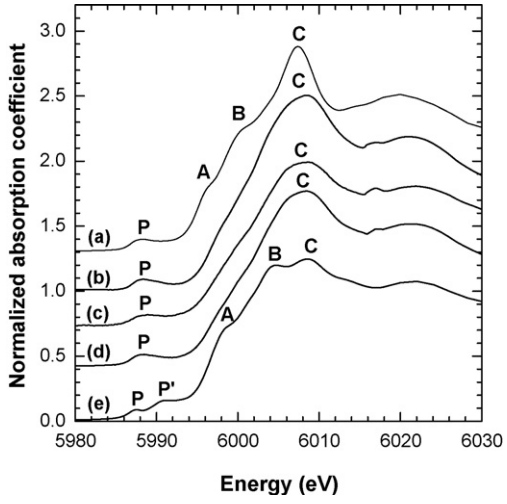

Fig. 5. Cr K-edge XANES spectra for (a) the precursor spinel $LiMn_{1.5}Cr_{0.5}O_4$ and their hydrothermally treated derivatives at (b) 120 °C, (c) 160 °C, (d) 180 °C, and (e) Cr_2O_3.

3.4. Electrochemical measurements

To investigate the influences of crystal structure and chromium substitution on the performance of the 1D nanostructured manganese oxides as electrode for lithium ion batteries, we have tested several selected samples. The relationship between the crystal structure and electrode activity of the 1D nanostructured manganates was examined by measuring the electrochemical property of the β-MnO_2-structured sample, the mixed α-MnO_2/β-MnO_2-structured sample, and the α-MnO_2-structured sample. These samples correspond to the 160 °C-hydrothermally treated $LiMn_{2-x}Cr_xO_4$ precursors with x = 0, 0.1, and 0.5, respectively. Also, the effect of Cr substitution on the electrode property was probed by measuring the electrode functionality of unsubstituted β-MnO_2 and Cr-substituted β-MnO_2 samples prepared at 180 °C with the precursors $LiMn_{2-x}Cr_xO_4$ with x = 0 and 0.1, respectively. As plotted in Fig. 6, all the present nanostructured manganates display a narrow plateau for the charging and discharging processes, which is characteristic of nanocrystalline electrode materials [22,24]. All of these materials show very high Coulombic efficiency of ~95–100%, reflecting the good stability of their electrochemical charge–discharge process.

The discharge capacities of the 1D nanostructured manganese oxides are plotted in Fig. 7 as a function of cycle number. Among the manganese oxides prepared at 160 °C, the β-MnO_2-structured material exhibits the best electrode performance for the entire cycles presented here, strongly suggesting the advan-

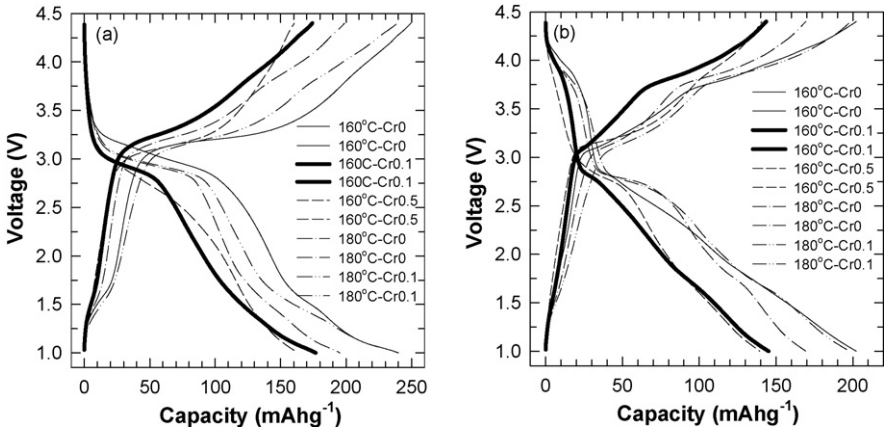

Fig. 6. Potential profiles of 1D nanostructured manganese oxides prepared by hydrothermal treatment for the precursors $LiMn_{2-x}Cr_xO_4$ with $x = 0$, 0.1, and 0.5 at 160 °C, and with $x = 0$ and 0.1 at 180 °C for (a) 2nd and (b) 30th cycle. The applied current condition is 20 mA g^{-1}.

Table 1
Effects of the synthesis temperature and chemical composition of precursors on the crystal structure and crystallite morphology of the resulting nanostructured manganese oxides.

Synthesis temperature (°C)	Cr content (x) in the precursors $LiMn_{2-x}Cr_xO_4$			
	0	0.1	0.3	0.5
120	α-/γ-MnO_2 nanowires	α-/γ-MnO_2 nanowires	α-/γ-MnO_2 nanowires	α-/γ-MnO_2 nanowires
160	β-MnO_2 nanorods	β-/α-MnO_2 nanorods	α-MnO_2 nanowires	α-MnO_2 nanowires
180	β-MnO_2 nanorods	β-MnO_2 nanorods	α-MnO_2 nanowires	α-MnO_2 nanowires

tage of β-MnO_2 structure in improving the electrode performance of nanostructured manganese oxides. According to ^{7}Li magic angle spinning-nuclear magnetic resonance, or MAS-NMR, spectroscopy [25], the electrochemical activity of the β-MnO_2 nanorods originates from the surface adsorption of Li^+ ions. This adsorption mechanism in the β-MnO_2 phase is quite different from the Li intercalation mechanism in the tunnel-structured α-MnO_2 phase. Thus, the formation of nanostructure with the expansion of surface area enhances more efficiently the electrode performance of the β-MnO_2 phase than that of the α-MnO_2 phase. This fact accounts for the observed superior performance of the β-MnO_2 nanorods to the α-MnO_2 nanowires (Fig. 7). Between the manganese oxides prepared at 180 °C, the Cr-substituted β-MnO_2 nanorod displays better electrode performance than the unsubstituted β-MnO_2 nanorod. This finding clearly demonstrates that the substitution of chromium ions is very useful for enhancing the electrochemical properties of 1D nanostructured manganese oxides. Such a positive effect of the Cr substitution is attributable to the high stability of CrO_6 octahedra during electrochemical cycling and to the resulting increase of the structural stability of manganate lattice [18]. In addition, Cr K-edge XANES results indicated that the substituted chromium ions have trivalent oxidation state (Fig. 5). The substitution of Mn^{3+}/Mn^{4+} ions with Cr^{3+} ions increases average Mn oxidation state and hence decreases the concentration of unstable Mn^{3+} ions [26]. Hence, the increase of Mn oxidation state caused by the Cr substitution makes another contribution to the improved electrochemical performance of the Cr-substituted manganese oxide nanorods. Despite the positive effect of Cr substitution, the Cr-substituted β-MnO_2 nanorod prepared at 180 °C shows nearly identical electrode performance to the unsubstituted β-MnO_2 nanorod prepared at 160 °C. This finding suggests that the elevation of synthesis temperature has negative effect on the electrode activity of the β-MnO_2 nanorods. The disadvantage of high synthesis temperature is related to the depression of the surface area of the nanorods by the enhanced agglomeration of crystal grains. As mentioned above, the increase of surface area is very crucial in optimizing the discharge capacity of the β-MnO_2 phase [25]. Taking into consideration, we tried to synthesize the β-MnO_2 nanorods at lower temperature of 140 °C but the reaction at this temperature produced the α-MnO_2 nanowires instead of the β-MnO_2 nanorods.

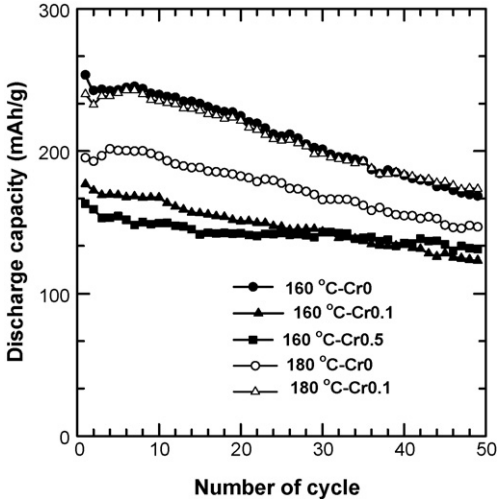

Fig. 7. Discharge capacity plots of 1D nanostructured manganese oxides prepared by hydrothermal treatment for the precursors $LiMn_{2-x}Cr_xO_4$ with $x = 0$, 0.1, and 0.5 at 160 °C, and with $x = 0$ and 0.1 at 180 °C. The applied current condition is 20 mA g^{-1}.

4. Conclusions

We successfully synthesized the 1D nanostructured manganese oxides with various crystal structures and morphologies by the treatments of microcrystalline $LiMn_{2-x}Cr_xO_4$ with persulfate under hydrothermal condition. As listed in Table 1, the crystal structure and crystallite morphology of the 1D nanostructured manganese oxides can be effectively controlled by the tuning of reaction temperature and the Cr substitution of the precursors. Both the

lowering of reaction temperature and the increase of Cr content in the precursors favor the formation of the α-MnO_2-structured nanowires. Conversely, both the elevation of reaction temperature and the decrease of Cr content commonly result in the formation of β-MnO_2 nanorods with a lower aspect ratio. The structural transformation into the β-MnO_2 phase and the partial substitution of Mn with Cr are advantageous for the optimization of the electrode performance of 1D nanostructured manganese oxides. In conclusion, the control of synthesis temperature and precursor composition can provide an effective way to tailor the crystal structure, morphology, and electrochemical performance of 1D nanostructured manganese oxides.

Acknowledgments

This work was supported by the General R/D Program of the Daegu Gyeongbuk Institute of Science and Technology (DGIST) funded by the Ministry of Education, Science and Technology (MEST) of the Republic of Korea, by a grant (20070401034003) from the BioGreen 21 Program, and by the Korea Science and Engineering Foundation (KOSEF) grant funded by the Korea government (MEST) (grant: 2008-0061493). The experiments at Pohang Accelerator Laboratory (PAL) were supported in part by MOST and POSTECH.

References

[1] M.M. Thackeray, Prog. Solid State Chem. 25 (1997) 1–71.
[2] P. Poizot, S. Laruelle, S. Grugeon, L. Dupont, J.-M. Tarascon, Nature 407 (2000) 496–499.
[3] A.R. Armstrong, G. Armstrong, J. Canales, R. García, P.G. Bruce, Adv. Mater. 17 (2005) 862–865.
[4] A.S. Arico, P. Bruce, B. Scrosati, J.-M. Tarascon, W.V. Schalkwijk, Nat. Mater. 4 (2005) 366–377.
[5] A. Singhal, G. Skandan, G. Amatucci, F. Badway, N. Ye, A. Manthiram, H. Ye, J.J. Xu, J. Power Sources 129 (2004) 38–44.
[6] J. Yuan, W.-N. Li, S. Gomez, S.L. Suib, J. Am. Chem. Soc. 127 (2005) 14184–14185.
[7] X. Wang, Y. Li, J. Am. Chem. Soc. 124 (2002) 2880–2881.
[8] X. Wang, Y. Li, Chem. Eur. J. 9 (2003) 300–306.
[9] D.H. Park, S.T. Lim, S.-J. Hwang, C.-S. Yoon, Y.K. Sun, J.-H. Choy, Adv. Mater. 17 (2005) 2834–2837.
[10] D.H. Park, S.-H. Lee, T.W. Kim, S.T. Lim, S.-J. Hwang, Y.S. Yoon, Y.H. Lee, J.-H. Choy, Adv. Funct. Mater. 17 (2007) 2949–2956.
[11] S.H. Lee, T.W. Kim, D.H. Park, J.-H. Choy, S.-J. Hwang, N. Jiang, S.E. Park, Y.H. Lee, Chem. Mater. 19 (2007) 5010–5017.
[12] D.H. Park, H.-W. Ha, S.H. Lee, J.-H. Choy, S.-J. Hwang, J. Phys. Chem. C 112 (2008) 5160–5164.
[13] B. Li, G. Rong, Y. Xie, L. Huang, C. Feng, Inorg. Chem. 45 (2006) 6404–6410.
[14] S.-J. Hwang, H.-S. Park, J.-H. Choy, G. Campet, J. Phys. Chem. B 105 (2001) 335–342.
[15] J.-H. Choy, S.-J. Hwang, N.-G. Park, J. Am. Chem. Soc. 119 (1997) 1624–1633.
[16] D.H. Park, S.T. Lim, S.-J. Hwang, J.-H. Choy, J.H. Choi, J. Choo, J. Power Sources 159 (2006) 1346–1352.
[17] In hydrothermal synthesis at higher temperature of 220 °C, the products show the same dependence of crystal structure on the Cr content in the precursors.
[18] S.-J. Hwang, H.S. Park, J.-H. Choy, G. Campet, J. Phys. Chem. B 104 (2000) 7612–7618.
[19] B. Deng, H. Nakamura, M. Yoshio, Electrochem. Solid-State Lett. 8 (2005) A171–A174.
[20] Estimated Cr/Mn ratios of the nanostructured manganese oxides prepared from the precursors $LiMn_{2x}Cr_xO_4$; 0.01 (120 °C), 0.01 (160 °C), and 0.02 (180 °C) for $x = 0.1$; 0.05 (120 °C), 0.02 (160 °C), and 0.07 (180 °C) for $x = 0.3$; 0.05 (120 °C), 0.05 (160 °C) and 0.09 (180 °C) for $x = 0.5$.
[21] R.D. Shannon, Acta Crystallogr. A 32 (1976) 751–767.
[22] S.-J. Hwang, C.-W. Kwon, J. Portier, G. Campet, H.-S. Park, J.-H. Choy, P.V. Huong, M. Yoshimura, M. Kakihana, J. Phys. Chem. B 106 (2002) 4053–4060.
[23] A. Manceau, A.I. Gorshkov, V.A. Drits, Am. Mineral. 77 (1992) 1133–1143.
[24] M. Okubo, E. Hosono, J. Kim, M. Enomoto, N. Kojima, T. Kudo, H. Zhou, I. Honma, J. Am. Chem. Soc. 129 (2007) 7444–7452.
[25] I.Y. Kim, H.-W. Ha, T.W. Kim, Y. Paik, J.-H. Choy, S.-J. Hwang, J. Phys. Chem. C (2009), web-published.
[26] M.M. Thackeray, M.F. Mansuetto, J.B. Bates, J. Power Sources 68 (1997) 153–158.